

Article

Influence of Growth Velocity on the Separation of Primary Silicon in Solidified Al-Si Hypereutectic Alloy Driven by a Pulsed Electric Current

Yunhu Zhang ^{1,*}, Chunyang Ye ¹, Yanyi Xu ¹, Honggang Zhong ^{2,*}, Xiangru Chen ¹,
Xincheng Miao ³, Changjiang Song ¹ and Qijie Zhai ¹

¹ State Key Laboratory of Advanced Special Steels, Shanghai Key Laboratory of Advanced Ferrometallurgy, School of Materials Science and Engineering, Shanghai University, Shanghai 200072, China; 18717923821@163.com (C.Y.); xuyanyi@i.shu.edu.cn (Y.X.); cxr16@shu.edu.cn (X.C.); riversxia@163.com (C.S.); qjzhai@shu.edu.cn (Q.Z.)

² Shanghai Institute of Materials Genome, Shanghai 200444, China

³ School of Materials Science and Engineering, University of Science and Technology Liaoning, Anshan 114051, China; miao-xincheng@hotmail.com

* Correspondence: zhangyunhu.zyh@163.com (Y.Z.); hgzhong@shu.edu.cn (H.Z.); Tel.: +86-21-5633-4045 (Y.Z.)

Academic Editor: Nong Gao

Received: 24 March 2017; Accepted: 5 May 2017; Published: 23 May 2017

Abstract: Investigating the separation of the primary silicon phase in Al-Si hypereutectic alloys is of high importance for the production of solar grade silicon. The present paper focuses on the effect of growth velocity on the electric current pulse (ECP)-induced separation of primary silicon in a directionally solidified Al-20.5 wt % Si hypereutectic alloy. Experimental results show that lower growth velocity promotes the enrichment tendency of primary silicon at the bottom region of the sample. The maximum measured area percentage of segregated primary silicon in the sample solidified at the growth velocity of 4 $\mu\text{m/s}$ is as high as 82.6%, whereas the corresponding value is only 59% in the sample solidified at the growth velocity of 24 $\mu\text{m/s}$. This is attributed to the fact that the stronger forced flow is generated to promote the precipitation of primary silicon accompanied by a higher concentration of electric current in the mushy zone under the application of a slower growth velocity.

Keywords: Al-Si hypereutectic alloy; growth velocity; separation of primary silicon; solidification; electric current pulse

1. Introduction

The production of solar grade silicon (SOG-Si) is of high commercial importance for the development of the silicon solar cell industry. The conventional process to manufacture SOG-Si is with modified Siemens technology. However, it is an expensive and pollution-heavy chemical process, although the quality of the manufactured SOG-Si is high. In order to overcome the cost and pollution issues, more efficient and low-cost metallurgical processes are employed to achieve SOG-Si from metallurgical grade silicon (MG-Si), such as vacuum refining [1], slag refining [2,3], directional solidification [4,5], plasma refining [6], electron beam melting [7,8], solvent refining [9], and so on.

Recently, Al-Si solvent refining has been intensively studied on account of the fact that the target silicon is purified more economically and efficiently [9,10]. It has been demonstrated that the precipitated primary silicon can be significantly purified as the melted Al-Si hypereutectic alloys solidify, because the segregation coefficient of most impurities can be dramatically decreased in Al-Si melt rather than in Si melt. The purified primary silicon as well as the target silicon is selectively collected via

acid leaching [10]. However, the acid leaching procedure results in considerable consumptions of Al in addition to the acid solution. Hence, in order to reduce these consumptions, it is important to develop methods to separate primary silicon from Al-Si melt or to allow the primary silicon to segregate at some special position within sample.

Electromagnetic fields present a strong ability to influence the solidification process of alloys [11,12], and have shown the potential to efficiently separate primary silicon from Al-Si melt during the solidification process, through methods such as electromagnetic stirring [13,14] and electric currents [15,16]. Jie et al. [13] showed that a rotating magnetic field can efficiently segregate the primary silicon to 65–69.8 wt % in hypereutectic Al-30 wt % Si alloy. Moreover, our results showed that the primary silicon phase also can be intensely separated by solely applying an electric current [16]. The area percentage of the aggregated primary silicon can be as high as 62.7% in Al-20.5 wt % Si alloy under the application of an electric current. The similar separation mechanism of primary silicon was proposed for Al-Si alloys influenced by electromagnetic stirring or electric currents. The Si-rich melt transferred by the magnetic or current-induced forced flow promotes the growth of the firstly precipitated primary silicon phase, while the rejected aluminum was relatively delivered to the bulk melt.

According to the proposed separation mechanism of primary silicon, the growth velocity of samples would be a crucial factor to influence the separation efficiency of primary silicon under the application of electric currents. Unfortunately, little attention has been paid to this parameter in previous research. One of the possible reasons for this is that the growth velocity is gradually varied in the case of traditional mold casting. In the present paper, the separation of primary silicon caused by a pulsed electric current is investigated under different growth velocities. In order to achieve a controllable growth velocity, the Bridgman furnace is employed to solidify the Al-Si hypereutectic alloy.

2. Materials and Methods

A schematic view of the experimental setup is shown in Figure 1. The Al-20.5 wt % Si hypereutectic alloy (nominal composition) was prepared by melting pure Al (99.9 wt %) and Si (99.9 wt %). In order to homogenize the solute elements, the melt was mechanically stirred and then sucked into a quartz tube (inner diameter in 4 mm) and cooled in ambient air. The melt in the quartz tube can be rapidly solidified because the diameter is only 4 mm. Hence, the homogeneity of solute elements in the sample scale is guaranteed. Then, the preparatory sample was embedded into an alumina crucible (420 mm in length and 4 mm in inner-diameter), and was vertically positioned at the central axis of the cylindrical Bridgman furnace (see Figure 1). The bottom end of the sample was connected to the downward pulling rod (stainless steel). The top end of the sample and pulling rod were respectively linked by two cables (copper) to conduct the electric current through the sample. After that, the furnace was heated up to 1173 K, and then held for 20 min to sufficiently remelt the middle part of sample. In view of the fact that the bottom part of the sample was immersed into the coolant (GaInSn liquid metal), a positive temperature gradient (about 35 K/mm) was constantly produced in the sample along the vertical direction. In the final step, the sample was pulled downwards at a speed of 4 and 24 $\mu\text{m/s}$, respectively. Meanwhile, a damping electric current pulse was initiated. The applied electric current intensity (I_p), frequency (f) and pulse length (t_p) were 400 A, 200 Hz and 0.5 ms, respectively. The waveform of the ECP is shown in Figure 2. The solidified sample was quenched into the coolant until the sample was solidified at the length of 8.5 cm.

Directionally solidified samples were cut along the longitudinal and transverse sections for metallographic examination. Selected sections were ground on SiC paper and then polished from 6 μm to 1 μm gradually. The as-polished samples were directly examined using optical microscopy. In order to quantify the distribution of primary silicon, the area percentage of the primary silicon in the transversal section was measured by using the software package ANALYSIS FIVE (Olympus Europe, Hamburg, Germany).

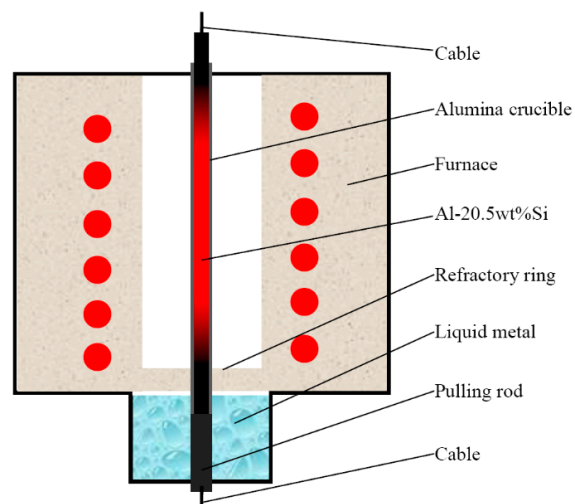


Figure 1. Schematic view of the solidification setup.

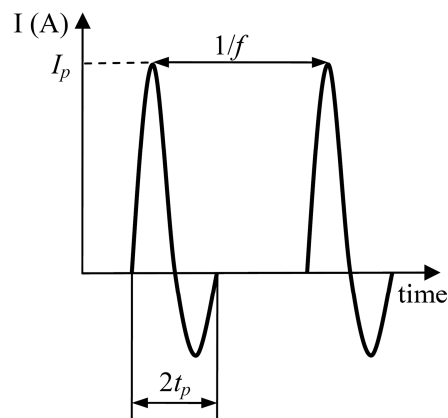


Figure 2. Waveform of the applied electric current pulse.

3. Results

The homogeneity of solute elements in the original sample was examined firstly. Figure 3 shows micrographs in the longitudinal section of the original sucked samples. It can be seen that the structures of the original Al-Si hypereutectic alloys consist of randomly distributed primary silicon and a eutectic structure.

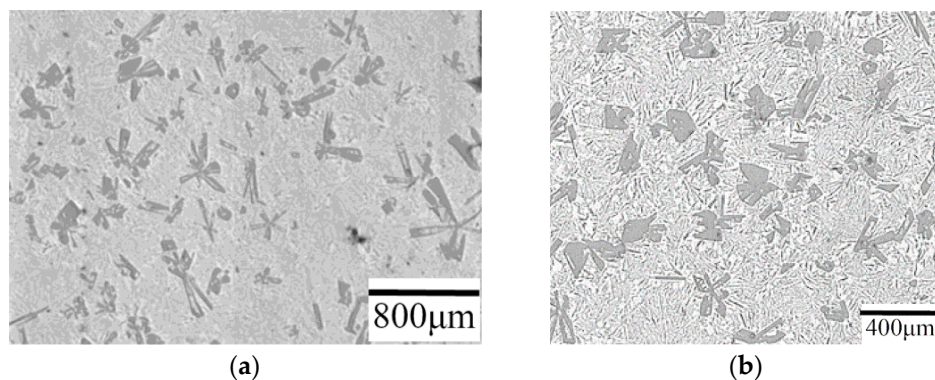


Figure 3. Micrographs in the different longitudinal sections of the original sucked sample at different zoom scales; (a) small; (b) large.

Figure 4 displays the solidified structure in the transversal section of the samples directionally solidified at the growth velocity of $4 \mu\text{m/s}$ and $24 \mu\text{m/s}$, respectively. The primary silicon distribution is reflected by the quantity evolution of the primary silicon phase in a series of transversal sections at the growth length of 1 cm, 2 cm, 4 cm, 6 cm and 8 cm. The distinct segregation of primary silicon at the bottom region can be observed no matter which growth velocity is applied. In addition, the quantity of primary silicon shows a slight increase tendency among the following growth regions of 4 cm–8 cm. However, the quantity of primary silicon in this region is far less than that in the segregated region. This indicates that most of the primary silicon can be selectively collected from the bottom segregated region of the sample.

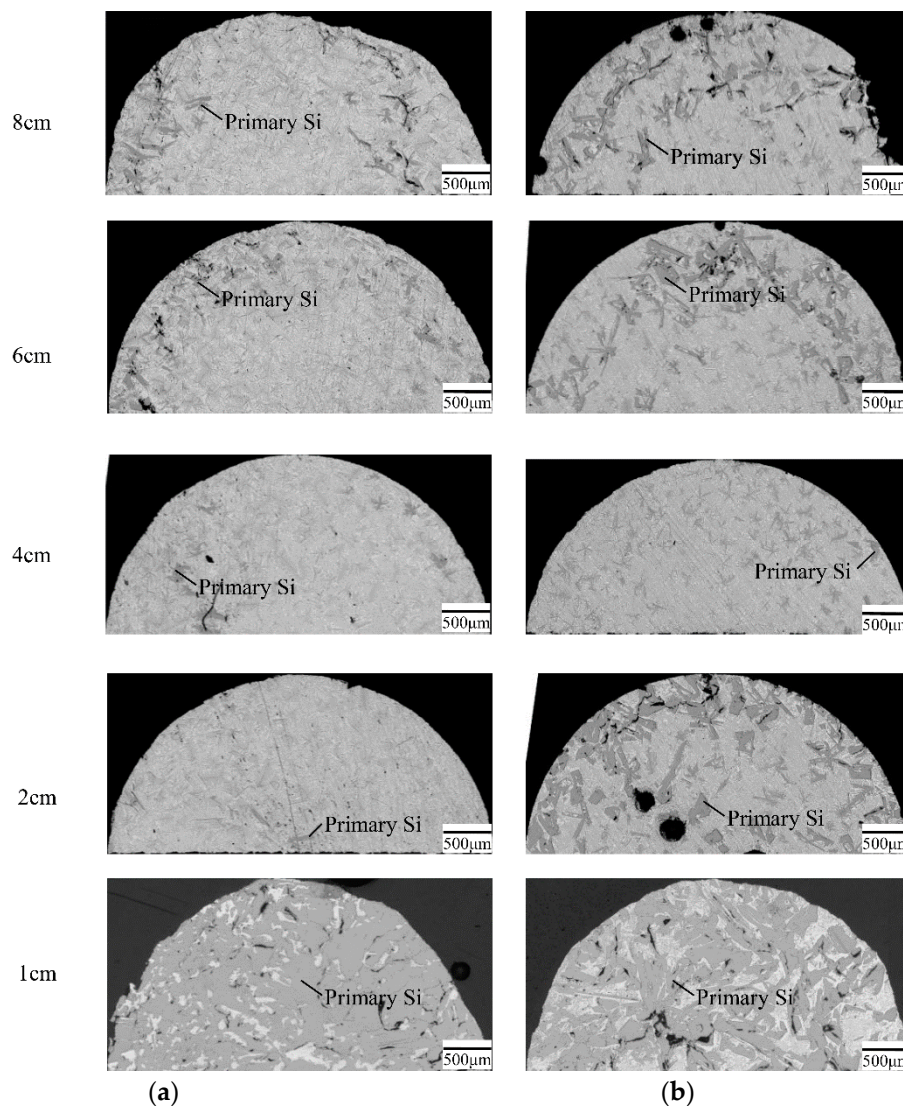


Figure 4. Solidified structure of Al-Si alloys with a conducted electric current pulse (ECP) on transversal sections at different growth lengths: (a) $4 \mu\text{m/s}$; (b) $24 \mu\text{m/s}$.

However, the quantity of the segregated primary silicon phase is significantly influenced by the employed growth velocity. As the solidified structures show in Figure 4, it is most likely that the segregation tendency of the primary silicon at the bottom region is remarkably reduced in the sample with higher growth velocity. The phase fraction can be achieved by using X-ray diffraction to identify the phase distribution [17,18]. However, the primary silicon phase and eutectic silicon phase cannot be classified. Hence, the area percentage of the primary silicon phase was measured to quantitatively

show the distribution of the primary silicon phase. Figure 5 presents the measured area percentage of primary silicon in the corresponding transversal sections. The value of the area percentage of primary silicon in sample solidified at the growth velocity of 4 $\mu\text{m/s}$ is as high as 82.6% at the growth length of 1 cm, whereas the value at the same growth length is decreased to 59% for the sample solidified at the growth velocity of 24 $\mu\text{m/s}$. When the growth length increases to 2 cm, the quantity of primary silicon is only 0.7% at the growth velocity of 4 $\mu\text{m/s}$. Yet, the area percentage of 23.8% still can be observed in the sample solidified at the growth velocity of 24 $\mu\text{m/s}$. This means that more primary silicon can be expected to congregate at the bottom region with the shorter length, when a slower growth velocity is employed.

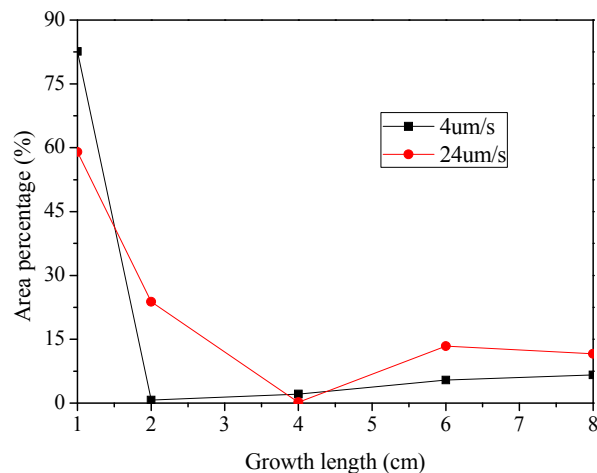


Figure 5. Measured area percentage of primary silicon in transversal sections of Al-Si hypereutectic alloy solidified at growth velocities of 4 $\mu\text{m/s}$ and 24 $\mu\text{m/s}$.

4. Discussion

A mechanism has been proposed to understand the occurrence of the intensely aggregated primary silicon phase in the initial growth region under the application of an ECP [16]. The primary silicon phase is firstly precipitated in the mushy zone during the directional solidification of Al-Si hypereutectic alloy. Since the electric conductivity of primary silicon is far less than that of the surrounding melt, the higher electric current intensity will result in the melt when the ECP is flowing through the mushy zone. The non-homogeneous distribution of electric currents can cause a strong forced flow inside the bulk melt due to the concentration of the electromagnetic force in the mushy zone among the primary silicon mushy zone. The forced flow can efficiently replace the depletion zone (Al-rich) surrounding the primary silicon by the Si-rich melt to cause the precipitation and segregation of primary silicon in the initial growth region. Moreover, the contribution of buoyancy forces to the segregation of primary silicon can be excluded, because the silicon particles should float upward and segregate at the top region rather than the observed bottom region under the influence of buoyancy forces, on account of the fact that silicon particles show less density than the bulk melt.

According to this mechanism, the quantity of the aggregated primary silicon can be influenced by the growth velocity. The lower growth velocity means that the electric current-induced forced flow will have more time to transport and exchange the silicon element to support the primary silicon growth. In addition, since the electric conductivity of the silicon phase is far less than that of the aluminum phase, the formed primary silicon with higher quantity at the lower growth velocity will generate a higher electric current intensity inside the melt among the primary silicon phase, which will give rise to a higher flow intensity, as schematically shown in Figure 6. The stronger forced flow enhances the silicon element exchange between the mushy zone and the bulk melt, which will further promote the segregation of the primary silicon (see Figure 6c,d). This is the reason why the primary silicon is

aggregated in a shorter region with an area percentage as high as 82.6% when the lower growth rate of $4 \mu\text{m/s}$ is applied.

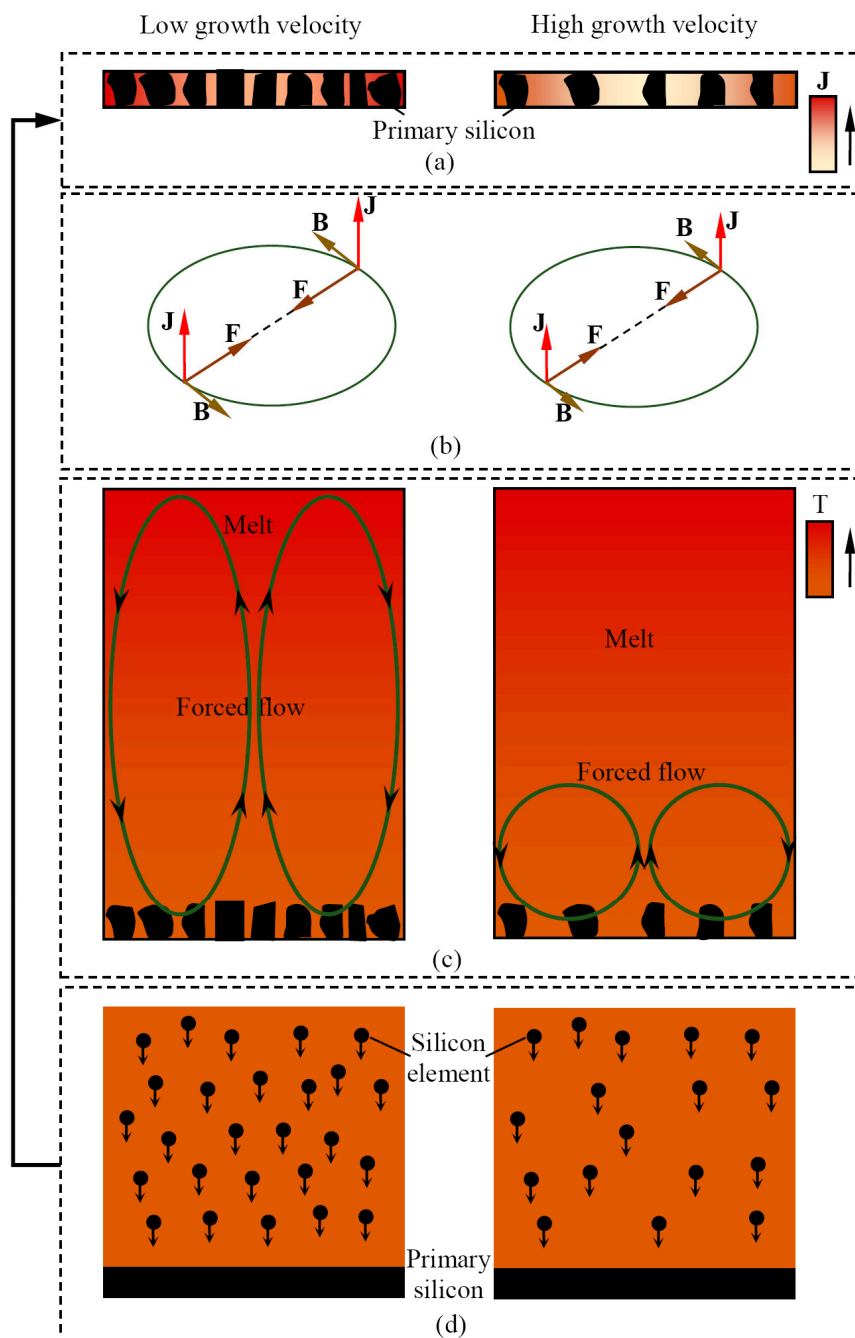


Figure 6. Schematic view of the primary silicon segregation mechanism under different growth velocities: (a) electric current density (J) distribution; (b) induced magnetic intensity (B) and Lorentz force (F); (c) forced flow inside melt (T : temperature); (d) silicon element transportation for primary silicon precipitation.

The present paper shows that the segregation quantity of the primary silicon phase can be profoundly influenced by solely varying the growth velocity. This implies that the growth velocity is a crucial factor to control the segregation of primary silicon under the application of the electric current. Moreover, it should be noted that although the directional solidification is employed in our present research, the achieved results are also representative of other solidification configurations. In addition,

the gained knowledge provides more insight into controlling the production of solar grade silicon under the influence of electric currents or magnetic fields. The optimized production of solar grade silicon should consider and couple both the influences of the parameters of solidification and applied electromagnetic fields.

5. Conclusions

This work investigates the influence of growth velocities on the separation of primary silicon in the directionally solidified Al-Si hypereutectic alloy under the application of a pulsed electric current (ECP). The severe segregation of primary silicon at the bottom region can be caused by an ECP in samples solidified at different growth velocities. However, the segregation tendency is significantly enhanced when a slower growth velocity is employed. This is because the slower growth velocity allows for the formation of more primary silicon phase, which can result in a forced flow with a higher intensity to promote the segregation of the primary silicon.

Acknowledgments: The authors gratefully acknowledge the financial supports from the Shanghai Sailing Program (Grant No. 17YF1405600), National Natural Science Foundation of China (Grant No. 51320105003, 51404150, 51227803), Science and Technology Commission of Shanghai Municipality (Grant No. 14DZ2261200).

Author Contributions: Yunhu Zhang, Honggang Zhong and Qijie Zhai conceived and designed the experiments; Yunhu Zhang, Chunyang Ye, Yanyi Xu performed the experiments; Yunhu Zhang, Xincheng Miao, Xiangru Chen, Changjiang Song analyzed and discussed the data; all authors contributed equally writing the paper.

Conflicts of Interest: The authors declare no conflict of interest.

Abbreviations

The following abbreviations are used in this manuscript:

ECP	Pulsed Electric Current
SG-Si	Solar Grade Silicon
MG-Si	Metallurgical Grade Silicon

References

1. Liu, K.; Wu, J.; Wei, K.; Ma, W.; Xie, K.; Li, S.; Yang, B.; Dai, Y. Application of molecular interaction volume model on removing impurity aluminum from metallurgical grade silicon by vacuum volatilization. *Vacuum* **2015**, *114*, 6–12. [[CrossRef](#)]
2. Wang, Y.; Ma, X.; Morita, K. Evaporation Removal of Boron from Metallurgical-Grade Silicon Using CaO-CaCl₂-SiO₂ Slag. *Metall. Mater. Trans. B* **2014**, *45*, 334–337. [[CrossRef](#)]
3. Ding, Z.; Ma, W.; Wei, K.; Wu, J.; Zhou, Y.; Xie, K. Boron removal from metallurgical-grade silicon using lithium containing slag. *J. Non-Cryst. Solids* **2012**, *358*, 2708–2712. [[CrossRef](#)]
4. Tan, Y.; Ren, S.; Shi, S.; Wen, S.; Jiang, D.; Dong, W.; Ji, M.; Sun, S. Removal of aluminum and calcium in multicrystalline silicon by vacuum induction melting and directional solidification. *Vacuum* **2014**, *99*, 272–276. [[CrossRef](#)]
5. Liu, T.; Dong, Z.; Zhao, Y.; Wang, J.; Chen, T.; Xie, H.; Li, J.; Ni, H.; Huo, D. Purification of metallurgical silicon through directional solidification in a large cold crucible. *J. Cryst. Growth* **2012**, *355*, 145–150. [[CrossRef](#)]
6. Alemany, C.; Trassy, C.; Pateyron, B.; Li, K.I.; Delannoy, Y. Refining of metallurgical-grade silicon by inductive plasma. *Sol. Energy Mater. Sol. Cells* **2002**, *72*, 41–48. [[CrossRef](#)]
7. Tan, Y.; Guo, X.; Shi, S.; Dong, W.; Jiang, D. Study on the removal process of phosphorus from silicon by electron beam melting. *Vacuum* **2013**, *93*, 65–70. [[CrossRef](#)]
8. Pires, J.C.S.; Otubo, J.; Braga, A.F.B.; Mei, P.R. The purification of metallurgical grade silicon by electron beam melting. *J. Mater. Process. Technol.* **2005**, *169*, 16–20. [[CrossRef](#)]
9. Wang, P.; Lu, H.; Lai, Y. Control of silicon solidification and the impurities from an Al-Si melt. *J. Cryst. Growth* **2014**, *390*, 96–100. [[CrossRef](#)]
10. Li, J.; Guo, Z. Thermodynamic evaluation of segregation behaviors of metallic impurities in metallurgical grade silicon during Al-Si solvent refining process. *J. Cryst. Growth* **2014**, *394*, 18–23. [[CrossRef](#)]

11. Zhang, Y.; Cheng, X.; Zhong, H.; Xu, Z.; Li, L.; Gong, Y.; Miao, X.; Song, C.; Zhai, Q. Comparative Study on the Grain Refinement of Al-Si Alloy Solidified under the Impact of Pulsed Electric Current and Travelling Magnetic Field. *Metals* **2016**, *6*, 170. [[CrossRef](#)]
12. Zhang, Y.; Rübiger, D.; Eckert, S. Solidification of pure aluminium affected by a pulsed electrical field and electromagnetic stirring. *J. Mater. Sci.* **2016**, *51*, 2153–2159. [[CrossRef](#)]
13. Jie, J.; Zou, Q.; Sun, J.; Lu, Y.; Wang, T.; Li, T. Separation mechanism of the primary Si phase from the hypereutectic Al-Si alloy using a rotating magnetic field during solidification. *Acta Mater.* **2014**, *72*, 57–66. [[CrossRef](#)]
14. Zou, Q.; Jie, J.; Sun, J.; Wang, T.; Cao, Z.; Li, T. Effect of Si content on separation and purification of the primary Si phase from hypereutectic Al-Si alloy using rotating magnetic field. *Sep. Purif. Technol.* **2015**, *142*, 101–107. [[CrossRef](#)]
15. Li, J.; Ni, P.; Wang, L.; Tan, Y. Influence of direct electric current on solidification process of Al-Si alloy. *Mater. Sci. Semicond. Process.* **2017**, *61*, 79–84. [[CrossRef](#)]
16. Zhang, Y.; Miao, X.; Shen, Z.; Han, Q.; Song, C.; Zhai, Q. Macro segregation formation mechanism of the primary silicon phase in directionally solidified Al-Si hypereutectic alloys under the impact of electric currents. *Acta Mater.* **2015**, *97*, 357–366. [[CrossRef](#)]
17. Zhang, L.C.; Das, J.; Lu, H.B.; Duhamel, C.; Calin, M.; Eckert, J. High strength Ti-Fe-Sn ultrafine composites with large plasticity. *Scr. Mater.* **2007**, *57*, 101–104. [[CrossRef](#)]
18. Ehtemam-Haghighi, S.; Liu, Y.; Cao, G.; Zhang, L.C. Phase transition, microstructural evolution and mechanical properties of Ti-Nb-Fe alloys induced by Fe addition. *Mater. Des.* **2016**, *97*, 279–286. [[CrossRef](#)]



© 2017 by the authors. Licensee MDPI, Basel, Switzerland. This article is an open access article distributed under the terms and conditions of the Creative Commons Attribution (CC BY) license (<http://creativecommons.org/licenses/by/4.0/>).